

$\bar{B} \rightarrow X_s \gamma$ in BLMSSM*

Jian-bin Chen^{1*}, Meng Zhang¹, Li-Li Xing^{1†},
Tai-Fu Feng^{2‡}, Shu-Min Zhao^{2§}, Ke-Sheng Sun^{3¶}

¹*College of Physics and Optoelectronic Engineering,*

Taiyuan University of Technology, Taiyuan 030024, China

²*Department of Physics, Hebei University, Baoding, 071002, China*

³*Department of Physics, Baoding University, Baoding, 071000, China*

Abstract

Applying the effective Lagrangian method, we study the Flavor Changing Neutral Current $b \rightarrow s\gamma$ within the minimal supersymmetric extension of the standard model where baryon and lepton numbers are local gauge symmetries. Constraints on the parameters are investigated numerically with the experimental data on branching ratio of $\bar{B} \rightarrow X_s \gamma$. Additionally, we present the corrections to direct CP-violation in $\bar{B} \rightarrow X_s \gamma$ and time-dependent CP-asymmetry in $B \rightarrow K^* \gamma$. With appropriate assumptions on parameters, we find the direct CP-violation A_{CP} is very small, while one-loop contributions to $S_{K^* \gamma}$ can be significant.

PACS numbers: 12.60.Jv; 12.15.Lk

Keywords: BLMSSM, Electroweak radiative corrections

¹ Supported by National Natural Science Foundation of China (11805140, 11347185 and 11905002), the Scientific and Technological Innovation Programs of Higher Education Institutions in Shanxi(20171113), Natural Science Foundation of Shanxi Province(201801D221021 and 201801D221031), Natural Science Foundation of Hebei Province(A2020201002), the China Scholarship Council(201906935031)

* chenjianbin@tyut.edu.cn

† xinglili@tyut.edu.cn

‡ fengtf@hbu.edu.cn

§ zhaosm@hbu.edu.cn

¶ sunkesheng@bdu.edu.cn

I. INTRODUCTION

Since the Flavor Changing Neutral Current process(FCNC) $b \rightarrow s\gamma$ originates only from loop diagrams, it is very sensitive to new physics beyond the Standard Model(SM). The updated average data of inclusive $\bar{B} \rightarrow X_s\gamma$ is [1]

$$BR(\bar{B} \rightarrow X_s\gamma)_{exp} = (3.40 \pm 0.21) \times 10^{-4}. \quad (1)$$

and the prediction of SM at next-next-to-leading order (NNLO) is[2–9]

$$BR(\bar{B} \rightarrow X_s\gamma)_{SM} = (3.36 \pm 0.23) \times 10^{-4}. \quad (2)$$

Though the deviation of SM prediction from experimental results has been almost eliminated in the past few years, it is helpful to constrain parameters of new physics.

The discovery of Higgs boson on Large Hadron Collider(LHC) makes SM the most successful theory in particle physics. Because of the hierarchy problem and missing of gravitational interaction, it is believed that SM is just an effective approximation of a more fundamental theory at higher scale. Among various extensions of SM, supersymmetric models have been studied for decades.

As the simplest extension, the Minimal Supersymmetric Standard Model(MSSM)[10] solves the hierarchy problem as well as the instability of Higgs boson by introducing a superpartner for each SM particle. The Lightest Supersymmetric Particle (LSP) within this framework also provides candidates of dark matter as Weakly Interacting Massive Particles (WIMPs). However the MSSM can not naturally generate tiny neutrino mass which is needed to explain the observation of neutrino oscillation. To acquire neutrino masses, heavy majorana neutrinos are introduced in the seesaw mechanism, which implies that the lepton numbers are broken. Besides, the baryon numbers are also expected to be broken because of the asymmetry of matter-antimatter in the universe. The authors of [11, 12] present the so called BLMSSM model in which the baryon and lepton number are local gauged and spontaneously broken at TeV scale. The experimental bounds on proton decay lifetime is the main motivation of great desert hypothesis. In BLMSSM, the proton decay can be avoided with discrete symmetry called matter parity and R-parity[13]

To describe the symmetries of baryon and lepton numbers, gauge group is enlarged to $SU(3)_C \otimes SU(2)_L \otimes U(1)_Y \otimes U(1)_B \otimes U(1)_L$. Then corrections to various observations

can be induced from new gauge boson and exotic fields within this scenario. In ref. [14], corrections to anomalous magnetic moment from one loop diagrams and two-loop Barr-Zee type diagrams are investigated with effective Lagrangian method. One-loop contributions to $c(t)$ electric dipole moment in CP-Violating BLMSSM is presented in ref. [15]. To account for the experimental data on Higgs, the authors of [16] study the signals of $h \rightarrow \gamma\gamma$ and $h \rightarrow VV^*(V = Z, W)$ with a 125 GeV Higgs. In this work, we use the branching ratio to constrain the parameters. Furthermore, we present the corrections to CP-Violation of $b \rightarrow s\gamma$ due to new parameters introduced in this model.

Our presentation is organized as follows. In section II, we briefly introduce the construction of BLMSSM and the interactions we need for our calculation. After that, we present the one-loop corrections to branching ratio and CP-Violation with effective Lagrangian method in section III. Numerical results are discussed in section IV and the conclusions is given in section V.

II. INTRODUCTION TO BLMSSM

The BLMSSM is based on gauge symmetry $SU(3)_C \otimes SU(2)_L \otimes U(1)_Y \otimes U(1)_B \otimes U(1)_L$. In order to cancel the anomalies of Baryon number(B), exotic quarks $\hat{Q}_4 \sim (3, 2, 1/6, B_4, 0)$, $\hat{U}_4^c \sim (\bar{3}, 1, -2/3, -B_4, 0)$, $\hat{D}_4^c \sim (\bar{3}, 1, 1/3, -B_4, 0)$, $\hat{Q}_5^c \sim (\bar{3}, 2, -1/6, -(1 + B_4), 0)$, $\hat{U}_5 \sim (3, 1, 2/3, 1 + B_4, 0)$, $\hat{D}_5 \sim (3, 1, -1/3, 1 + B_4, 0)$ are introduced. Baryon number are broken spontaneously after Higgs superfields $\hat{\Phi}_B \sim (1, 1, 0, 1, 0)$, $\hat{\varphi}_B \sim (1, 1, 0, -1, 0)$ acquire nonzero vacuum expectation values(VEVs). To deal with the anomalies of Lepton number(L), exotic leptons $\hat{L}_4 \sim (1, 2, -1/2, 0, L_4)$, $\hat{E}_4^c \sim (1, 1, 1, 0, -L_4)$, $\hat{N}_4^c \sim (1, 1, 0, 0, -L_4)$, $\hat{L}_5^c \sim (1, 2, 1/2, 0, -(3 + L_4))$, $\hat{E}_5 \sim (1, 1, -1, 0, 3 + L_4)$, $\hat{N}_5 \sim (1, 1, 0, 0, 3 + L_4)$ are introduced, and $\hat{\Phi}_L \sim (1, 1, 0, 0, -2)$, $\hat{\varphi}_L \sim (1, 1, 0, 0, 2)$ are responsible for the breaking of lepton number[12]. The superfields $\hat{X} \sim (1, 1, 0, 2/3 + B_4, 0)$, $\hat{X}' \sim (1, 1, 0, -(2/3 + B_4), 0)$ which mediate the decay of exotic quarks are added in this model to avoid their stability.

Given the superfields above, one can construct the superpotential as

$$\mathcal{W}_{BLMSSM} = \mathcal{W}_{MSSM} + \mathcal{W}_B + \mathcal{W}_L + \mathcal{W}_X, \quad (3)$$

where \mathcal{W}_{MSSM} indicates the superpotential of MSSM, and

$$\begin{aligned}
\mathcal{W}_B &= \lambda_Q \hat{Q}_4 \hat{Q}_5^c \hat{\Phi}_B + \lambda_U \hat{U}_4^c \hat{U}_5 \hat{\varphi}_B + \lambda_D \hat{D}_4^c \hat{D}_5 \hat{\varphi}_B + \mu_B \hat{\Phi}_B \hat{\varphi}_B \\
&\quad + Y_{u_4} \hat{Q}_4 \hat{H}_u \hat{U}_4^c + Y_{d_4} \hat{Q}_4 \hat{H}_d \hat{D}_4^c + Y_{u_5} \hat{Q}_5^c \hat{H}_d \hat{U}_5 + Y_{d_5} \hat{Q}_5^c \hat{H}_u \hat{D}_5, \\
\mathcal{W}_L &= Y_{e_4} \hat{L}_4 \hat{H}_d \hat{E}_4^c + Y_{\nu_4} \hat{L}_4 \hat{H}_u \hat{N}_4^c + Y_{e_5} \hat{L}_5^c \hat{H}_u \hat{E}_5 + Y_{\nu_5} \hat{L}_5^c \hat{H}_d \hat{N}_5 \\
&\quad + Y_\nu \hat{L} \hat{H}_u \hat{N}^c + \lambda_{N^c} \hat{N}^c \hat{N}^c \hat{\varphi}_L + \mu_L \hat{\Phi}_L \hat{\varphi}_L, \\
\mathcal{W}_X &= \lambda_1 \hat{Q} \hat{Q}_5^c \hat{X} + \lambda_2 \hat{U}^c \hat{U}_5 \hat{X}' + \lambda_3 \hat{D}^c \hat{D}_5 \hat{X}' + \mu_X \hat{X} \hat{X}'. \tag{4}
\end{aligned}$$

The soft breaking terms are given by

$$\begin{aligned}
\mathcal{L}_{soft} &= \mathcal{L}_{soft}^{MSSM} - (m_{\tilde{N}^c}^2)_{IJ} \tilde{N}_I^{c*} \tilde{N}_J^c - m_{\tilde{Q}_4}^2 \tilde{Q}_4^\dagger \tilde{Q}_4 - m_{\tilde{U}_4}^2 \tilde{U}_4^{c*} \tilde{U}_4^c - m_{\tilde{D}_4}^2 \tilde{D}_4^{c*} \tilde{D}_4^c \\
&\quad - m_{\tilde{Q}_5}^2 \tilde{Q}_5^{c\dagger} \tilde{Q}_5^c - m_{\tilde{U}_5}^2 \tilde{U}_5^{c*} \tilde{U}_5^c - m_{\tilde{D}_5}^2 \tilde{D}_5^{c*} \tilde{D}_5^c - m_{\tilde{L}_4}^2 \tilde{L}_4^\dagger \tilde{L}_4 - M_{\tilde{\nu}_4}^2 \tilde{\nu}_4^{c*} \tilde{\nu}_4^c - m_{\tilde{E}_4}^2 \tilde{e}_4^{c*} \tilde{e}_4^c \\
&\quad - m_{\tilde{L}_5}^2 \tilde{L}_5^{c\dagger} \tilde{L}_5^c - M_{\tilde{\nu}_5}^2 \tilde{\nu}_5^{c*} \tilde{\nu}_5^c - m_{\tilde{E}_5}^2 \tilde{e}_5^{c*} \tilde{e}_5^c - m_{\Phi_B}^2 \Phi_B^* \Phi_B - m_{\varphi_B}^2 \varphi_B^* \varphi_B \\
&\quad - m_{\Phi_L}^2 \Phi_L^* \Phi_L - m_{\varphi_L}^2 \varphi_L^* \varphi_L - (m_B \lambda_B \lambda_B + m_L \lambda_L \lambda_L + h.c.) \\
&\quad + \left\{ A_{u_4} Y_{u_4} \tilde{Q}_4 H_u \tilde{U}_4^c + A_{d_4} Y_{d_4} \tilde{Q}_4 H_d \tilde{D}_4^c + A_{u_5} Y_{u_5} \tilde{Q}_5^c H_d \tilde{U}_5 + A_{d_5} Y_{d_5} \tilde{Q}_5^c H_u \tilde{D}_5 \right. \\
&\quad + A_{BQ} \lambda_Q \tilde{Q}_4 \tilde{Q}_5^c \Phi_B + A_{BU} \lambda_U \tilde{U}_4^c \tilde{U}_5 \varphi_B + A_{BD} \lambda_D \tilde{D}_4^c \tilde{D}_5 \varphi_B + B_B \mu_B \Phi_B \varphi_B + h.c. \Big\} \\
&\quad + \left\{ A_{e_4} Y_{e_4} \tilde{L}_4 H_d \tilde{E}_4^c + A_{N_4} Y_{N_4} \tilde{L}_4 H_u \tilde{N}_4^c + A_{e_5} Y_{e_5} \tilde{L}_5^c H_u \tilde{E}_5 + A_{N_5} Y_{N_5} \tilde{L}_5^c H_d \tilde{N}_5 \right. \\
&\quad + A_N Y_N \tilde{L} H_u \tilde{N}^c + A_{N^c} \lambda_{N^c} \tilde{N}^c \tilde{N}^c \varphi_L + B_L \mu_L \Phi_L \varphi_L + h.c. \Big\} \\
&\quad + \left\{ A_1 \lambda_1 \tilde{Q} \tilde{Q}_5^c X + A_2 \lambda_2 \tilde{U}^c \tilde{U}_5 X' + A_3 \lambda_3 \tilde{D}^c \tilde{D}_5 X' + B_X \mu_X X X' + h.c. \right\}. \tag{5}
\end{aligned}$$

The first term $\mathcal{L}_{soft}^{MSSM}$ denotes the soft breaking terms of MSSM. To break the gauge symmetry from $SU(3)_C \otimes SU(2)_L \otimes U(1)_Y \otimes U(1)_B \otimes U(1)_L$ to electromagnetic symmetry $U(1)_e$, nonzero VEVs v_u, v_d and $v_B, \bar{v}_B, v_L, \bar{v}_L$ are allocated to $SU(2)_L$ doublets H_u, H_d and $SU(2)_L$ singlets $\Phi_B, \varphi_B, \Phi_L, \varphi_L$.

$$\begin{aligned}
H_u &= \begin{pmatrix} H_u^+ \\ (v_u + H_u^0 + iP_u^0)/\sqrt{2} \end{pmatrix}, \\
H_d &= \begin{pmatrix} (v_d + H_d^0 + iP_d^0)/\sqrt{2} \\ H_d^- \end{pmatrix}, \\
\Phi_B &= (v_B + \Phi_B^0 + iP_B^0)/\sqrt{2}, \\
\varphi_B &= (\bar{v}_B + \varphi_B^0 + i\bar{P}_B^0)/\sqrt{2}, \\
\Phi_L &= (v_L + \Phi_L^0 + iP_L^0)/\sqrt{2}, \\
\varphi_L &= (\bar{v}_L + \varphi_L^0 + i\bar{P}_L^0)/\sqrt{2}.
\end{aligned} \tag{6}$$

Here we take the notation $\tan \beta = v_u/v_d$, $\tan \beta_B = \bar{v}_B/v_B$ and $\tan \beta_L = \bar{v}_L/v_L$. After spontaneously breaking and unitary transformation from interactive eigenstate to mass eigenstate, one can extract the Feynman rules and mass spectrums in BLMSSM. The mass matrices of the particles that mediate the one-loop process $b \rightarrow s\gamma$ can be found in ref. [17]. The Feynman rules that we need can be extracted from the following terms, where all the repeated index of generation should be summed over.

$$\begin{aligned}
\mathcal{L}_{H^\pm du} &= \left(-Y_d^I Z_H^{1i} P_L + Y_u^J Z_H^{2i} P_R \right) K^{JI*} \bar{d}^I u^J H_i^\pm, \\
\mathcal{L}_{\tilde{D}\chi^0 d} &= \left[\left(\frac{-e}{\sqrt{2}s_W c_W} Z_D^{Ii} \left(\frac{1}{3} Z_N^{1j} s_W - Z_N^{2j} c_W \right) + Y_d^I Z_D^{(I+3)i} Z_N^{3j} \right) P_L \right. \\
&\quad \left. + \left(\frac{-e\sqrt{2}}{3c_W} Z_D^{(I+3)i} Z_N^{1j*} + Y_d^I Z_D^{Ii} Z_N^{3j*} \right) P_R \right] \bar{\chi}_j^0 d^I \tilde{D}_i^+, \\
\mathcal{L}_{\tilde{D}\chi_B^0 d} &= \frac{\sqrt{2}}{3} g_B \left(Z_{NB}^{1j} Z_D^{Ii} P_L + Z_{NB}^{1j*} Z_D^{(I+3)i} P_R \right) \bar{\chi}_{B_j}^0 d^I \tilde{D}^+, \\
\mathcal{L}_{\tilde{U}\chi^- d} &= \left[\left(\frac{-e}{s_W} Z_U^{Ji*} Z_+^{1j} + Y_u^J Z_U^{(J+3)i*} Z_+^{2j} \right) P_L - Y_d^I Z_U^{Ji*} Z_-^{2j*} P_R \right] K^{JI} \bar{\chi}^- d \tilde{U}^-, \\
\mathcal{L}_{Xb'd} &= \left[\lambda_1 (W_b^\dagger)_{j1} (Z_X)_{1k} P_L - \lambda_3^* (U_b^\dagger)_{j2} (Z_X)_{2k} P_R \right] \bar{b}'_j d^I X_k, \\
\mathcal{L}_{\tilde{b}'\tilde{X}d} &= - \left[\lambda_1 (W_{\tilde{b}'}^*)_{3\rho} P_L + \lambda_3^* (W_{\tilde{b}'})_{4\rho} P_R \right] \bar{\tilde{X}} d^I \tilde{b}'_\rho, \\
\mathcal{L}_{\tilde{D}\Lambda_G d} &= g_3 \sqrt{2} Y_{\alpha\beta}^a \left(-Z_D^{Ii} P_L + Z_D^{(I+3)i} P_R \right) \bar{\Lambda}_G^a d_\beta^I \tilde{D}_{i\alpha}^+.
\end{aligned} \tag{7}$$

III. ONE-LOOP CORRECTIONS TO $b \rightarrow s\gamma$ FROM BLMSSM

The flavor transition process $b \rightarrow s\gamma$ can be described by effective Hamiltonian at scale $\mu = O(m_b)$ as follow [18]:

$$\mathcal{H}_{eff}(b \rightarrow s\gamma) = -\frac{4G_F}{\sqrt{2}}V_{ts}^*V_{tb}\left[C_1Q_1^c + C_2Q_2^c + \sum_{i=3}^6 C_iQ_i + \sum_{i=7}^8 (C_iQ_i + \tilde{C}_i\tilde{Q}_i)\right], \quad (8)$$

and the operators are given by ref. [19–21]:

$$\begin{aligned} \mathcal{O}_1^c &= (\bar{s}_L\gamma_\mu T^a b_L)(\bar{c}_L\gamma^\mu T^a b_L), \\ \mathcal{O}_2^c &= (\bar{s}_L\gamma_\mu b_L)(\bar{c}_L\gamma^\mu T^a b_L), \\ \mathcal{O}_3 &= (\bar{s}_L\gamma_\mu b_L)\sum_q(\bar{q}\gamma^\mu q), \\ \mathcal{O}_4 &= (\bar{s}_L\gamma_\mu T^a b_L)\sum_q(\bar{q}\gamma^\mu T^a q), \\ \mathcal{O}_5 &= (\bar{s}_L\gamma_\mu\gamma_\nu\gamma_\rho b_L)\sum_q(\bar{q}\gamma^\mu\gamma^\mu\gamma^\nu\gamma^\rho q), \\ \mathcal{O}_6 &= (\bar{s}_L\gamma_\mu\gamma_\nu\gamma_\rho T^a b_L)\sum_q(\bar{q}\gamma^\mu\gamma^\mu\gamma^\nu\gamma^\rho T^a q), \\ \mathcal{O}_7 &= e/g_s^2 m_b(\bar{s}_L\sigma_{\mu\nu} b_R)F^{\mu\nu}, \\ \mathcal{O}_8 &= 1/g_s^2 m_b(\bar{s}_L\sigma_{\mu\nu} T^a b_R)G^{a,\mu\nu}, \\ \tilde{\mathcal{O}}_7 &= e/g_s^2 m_b(\bar{s}_R\sigma_{\mu\nu} b_L)F^{\mu\nu}, \\ \tilde{\mathcal{O}}_8 &= 1/g_s^2 m_b(\bar{s}_R\sigma_{\mu\nu} T^a b_L)G^{a,\mu\nu}. \end{aligned} \quad (9)$$

Coefficients of these operators can be extracted from Feynman amplitudes that originate from considered diagrams. Actually only the Coefficients of $\mathcal{O}_{7,8}$ and $\tilde{\mathcal{O}}_{7,8}$ are needed if we adopt the branching ratio formula presented in ref. [18]:

$$\begin{aligned} &BR(\bar{B} \rightarrow X_s\gamma)_{NP} \\ &= 10^{-4} \times \left\{ (3.36 \pm 0.23) + \frac{16\pi^2 a_{77}}{\alpha_s^2(\mu_b)} [|C_{7,NP}(\mu_{EW})|^2 + |\tilde{C}_{7,NP}(\mu_{EW})|^2] \right. \\ &\quad + \frac{16\pi^2 a_{88}}{\alpha_s^2(\mu_b)} [|C_{8,NP}(\mu_{EW})|^2 + |\tilde{C}_{8,NP}(\mu_{EW})|^2] \\ &\quad + \frac{4\pi}{\alpha_s(\mu_b)} \text{Re}[a_7 C_{7,NP}(\mu_{EW}) + a_8 C_{8,NP}(\mu_{EW}) \\ &\quad \left. + \frac{4\pi a_{78}}{\alpha_s(\mu_b)} (C_{7,NP}(\mu_{EW})C_{8,NP}(\mu_{EW}) + \tilde{C}_{7,NP}(\mu_{EW})\tilde{C}_{8,NP}(\mu_{EW}))] \right\}, \end{aligned} \quad (10)$$

where the first term is SM prediction. The others come from new physics in which $C_{7,NP}(\mu_{EW})$, $C_{8,NP}(\mu_{EW})$, $\tilde{C}_{7,NP}(\mu_{EW})$ and $\tilde{C}_{8,NP}(\mu_{EW})$ indicate Wilson coefficients at electroweak scale. It is an advantage of this expression that we don't have to evolve them down

to hadronic scale $\mu \sim m_b$ as the effect of evolution has already been involved in the coefficients $a_{7,8,77,88,78}$. The numerical values of these coefficients are given in table I.

TABLE I: Numerical values for the coefficients $a_{7,8,77,88,78}$ at electroweak scale.

a_7	a_8	a_{77}	a_{88}	a_{78}
$-7.184 + 0.612i$	$-2.225 - 0.557i$	4.743	0.789	$2.454 - 0.884i$

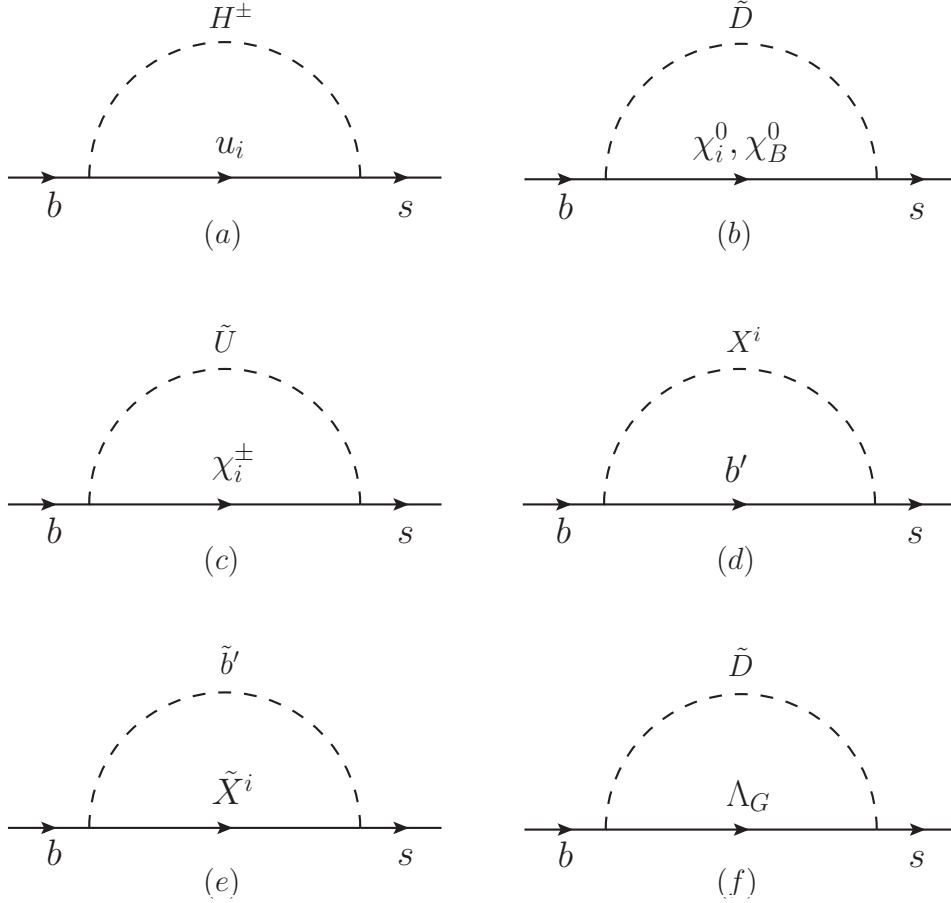


FIG. 1: One-loop Feynman diagrams of $b \rightarrow s$. The inner-line particles χ_B^0, X denote baryon neutralinos and new scalar particle introduced in BLMSSM. b' and \tilde{b}' are exotic quarks and squarks respectively. The photon and gluon can be attached in all possible ways.

To obtain the New Physics corrections in BLMSSM, we investigate one-loop diagrams shown in Figure 1. Photons should be attached to all inner lines with electric charge to complete the diagrams of $b \rightarrow s\gamma$ that contribute to \mathcal{O}_7 and $\tilde{\mathcal{O}}_7$. Similarly, diagrams of $b \rightarrow sg$ can be completed with gluons attached to all the inner lines with color charge, and

\mathcal{O}_8 and $\tilde{\mathcal{O}}_8$ originate from these process.

In details, we attach a photon to SM quark u_i , ($i = 1, 2, 3$) or charged Higgs H^\pm in Figure 1.(a) to get a set of trigonal diagrams for $b \rightarrow s\gamma$, while gluon can only be attached to up-type quarks u_i to form a specific diagram of $b \rightarrow sg$. To give a complete correction originating from Figure 1.(a), contributions from all generations of u_i and Higgs should be summed over. From the amplitudes of these diagrams, one can extract Wilson coefficients of electric- and chromomagnetic-dipole operators \mathcal{O}_7 and $\tilde{\mathcal{O}}_7$ at electroweak scale,

$$\begin{aligned} \frac{G_F}{\sqrt{2}} C_{7\gamma}^a(\Lambda) &= -i\Lambda^{-2}(V_{ts}^* V_{tb})^{-1} \left\{ (\eta_{H^\pm}^L)_{su_i}^\dagger (\eta_{H^\pm}^L)_{u_i b} F_{1,\gamma}^{(a)}(x_{u_i}, x_{H^\pm}) \right. \\ &\quad \left. + \frac{m_f}{m_b} (\eta_{H^\pm}^L)_{su_i}^\dagger (\eta_{H^\pm}^R)_{u_i b} F_{2,\gamma}^{(a)}(x_{u_i}, x_{H^\pm}) \right\}, \\ \frac{G_F}{\sqrt{2}} \tilde{C}_{7\gamma}^a(\Lambda) &= \frac{G_F}{\sqrt{2}} C_{7\gamma}^a(\Lambda) (\eta_{H^\pm}^L \leftrightarrow \eta_{H^\pm}^R), \end{aligned} \quad (11)$$

where $x_i = m_i^2/\mu_{EW}^2$. The concrete expressions of relevant couplings are already given in previous section, and the form factors can be written as:

$$\begin{aligned} F_{1,\gamma}^{(a)}(x, y) &= \left[\frac{1}{72} \frac{\partial^3 \varrho_{3,1}}{\partial y^3} + \frac{1}{24} \frac{\partial^2 \varrho_{2,1}}{\partial y^2} - \frac{1}{6} \frac{\partial \varrho_{1,1}}{\partial y} \right] (x, y), \\ F_{2,\gamma}^{(a)}(x, y) &= \left[\frac{1}{12} \frac{\partial^2 \varrho_{2,1}}{\partial y^2} - \frac{1}{6} \frac{\partial \varrho_{1,1}}{\partial y} - \frac{1}{3} \frac{\partial \varrho_{1,1}}{\partial x} \right] (x, y), \end{aligned} \quad (12)$$

where function $\varrho_{m,n}(x, y)$ is defined as:

$$\varrho_{m,n}(x, y) = \frac{x^m \ln^n x - y^m \ln^n y}{x - y}. \quad (13)$$

Corrections from all the other diagrams to $C_{7\gamma}$ and $\tilde{C}_{7\gamma}$ can be obtained similarly. In Figure 1.(b), the photon can only be attached to charged $-1/3$ squark \tilde{D} . We present contributions from both neutralinos χ_i^0 and baryon neutralinos χ_B^0 at electroweak scale as

$$\begin{aligned} \frac{G_F}{\sqrt{2}} C_{7\gamma}^b(\Lambda) &= -i\Lambda^{-2}(V_{ts}^* V_{tb})^{-1} \left\{ (\xi_{\chi_i^0}^L)_{s\tilde{D}}^\dagger (\xi_{\chi_i^0}^L)_{\tilde{D}b} F_{1,\gamma}^{(b)}(x_{\chi_i^0}, x_{\tilde{D}}) + \frac{m_f}{m_b} (\xi_{\chi_i^0}^L)_{s\tilde{D}}^\dagger (\xi_{\chi_i^0}^R)_{\tilde{D}b} F_{2,\gamma}^{(b)}(x_{\chi_i^0}, x_{\tilde{D}}) \right. \\ &\quad \left. + (\xi_{\chi_B^0}^L)_{s\tilde{D}}^\dagger (\xi_{\chi_B^0}^L)_{\tilde{D}b} F_{1,\gamma}^{(b)}(x_{\chi_B^0}, x_{\tilde{D}}) + \frac{m_f}{m_b} (\xi_{\chi_B^0}^L)_{s\tilde{D}}^\dagger (\xi_{\chi_B^0}^R)_{\tilde{D}b} F_{2,\gamma}^{(b)}(x_{\chi_B^0}, x_{\tilde{D}}) \right\}, \\ \frac{G_F}{\sqrt{2}} \tilde{C}_{7\gamma}^b(\Lambda) &= \frac{G_F}{\sqrt{2}} C_{7\gamma}^b(\Lambda) (\xi_{\chi_i^0}^L \leftrightarrow \xi_{\chi_i^0}^R, \xi_{\chi_B^0}^L \leftrightarrow \xi_{\chi_B^0}^R). \end{aligned} \quad (14)$$

$$\begin{aligned} F_{1,\gamma}^{(b)}(x, y) &= \left[-\frac{1}{72} \frac{\partial^3 \varrho_{3,1}}{\partial^3 y} + \frac{1}{24} \frac{\partial^2 \varrho_{2,1}}{\partial^2 y} \right] (x, y), \\ F_{2,\gamma}^{(b)}(x, y) &= \left[-\frac{1}{12} \frac{\partial^2 \varrho_{2,1}}{\partial^2 y} + \frac{1}{6} \frac{\partial \varrho_{1,1}}{\partial y} \right] (x, y). \end{aligned} \quad (15)$$

With the photon attached to the charged $+2/3$ squarks \tilde{U} or chargino χ_i^\pm in Figure 1.(c), the contributions to Wilson coefficients read

$$\begin{aligned}\frac{G_F}{\sqrt{2}}C_{7\gamma}^c(\Lambda) &= -i\Lambda^{-2}(V_{ts}^*V_{tb})^{-1}\left\{(\eta_{\tilde{U}}^L)^\dagger_{s\chi_i^\pm}(\eta_{\tilde{U}}^L)_{\chi_i^\pm b}F_{1,\gamma}^{(c)}(x_{\chi_i^\pm},x_{\tilde{U}})+\frac{m_f}{m_b}(\eta_{\tilde{U}}^L)^\dagger_{s\chi_i^\pm}(\eta_{\tilde{U}}^R)_{\chi_i^\pm b}F_{2,\gamma}^{(c)}(x_{\chi_i^\pm},x_{\tilde{U}})\right\}, \\ \frac{G_F}{\sqrt{2}}\tilde{C}_{7\gamma}^c(\Lambda) &= \frac{G_F}{\sqrt{2}}C_{7\gamma}^c(\Lambda)(\eta_{\tilde{U}}^L \leftrightarrow \eta_{\tilde{U}}^R).\end{aligned}\quad (16)$$

$$\begin{aligned}F_{1,\gamma}^{(c)}(x,y) &= \left[-\frac{1}{72}\frac{\partial^3\varrho_{3,1}}{\partial^3y}+\frac{1}{6}\frac{\partial^2\varrho_{2,1}}{\partial^2y}-\frac{1}{4}\frac{\partial\varrho_{1,1}}{\partial y}\right](x,y), \\ F_{2,\gamma}^{(c)}(x,y) &= \left[-\frac{1}{12}\frac{\partial^2\varrho_{2,1}}{\partial^2y}+\frac{1}{6}\frac{\partial\varrho_{1,1}}{\partial y}-\frac{1}{2}\frac{\partial\varrho_{1,1}}{\partial x}\right](x,y).\end{aligned}\quad (17)$$

The intermediate particles in Figure 1.(d) are the exotic quarks b' with charge $-1/3$ and superfield X introduced in BLMSSM. The contributions from this diagram are

$$\begin{aligned}\frac{G_F}{\sqrt{2}}C_{7\gamma}^d(\Lambda) &= -i\Lambda^{-2}(V_{ts}^*V_{tb})^{-1}\left\{(\eta_{X^j}^L)^\dagger_{sb'}(\eta_{X^j}^L)_{b'b}F_{1,\gamma}^{(d)}(x_{b'},x_{X^j})+\frac{m_f}{m_b}(\eta_{X^j}^L)^\dagger_{sb'}(\eta_{X^j}^R)_{b'b}F_{2,\gamma}^{(d)}(x_{b'},x_{X^j})\right\}, \\ \frac{G_F}{\sqrt{2}}\tilde{C}_{7\gamma}^d(\Lambda) &= \frac{G_F}{\sqrt{2}}C_{7\gamma}^d(\Lambda)(\eta_{X^j}^L \leftrightarrow \eta_{X^j}^R).\end{aligned}\quad (18)$$

Correspondingly, the corrections of exotic squarks \tilde{b}' with charge $-1/3$ and fermionic particle X can be obtained from Figure 1.(e)

$$\begin{aligned}\frac{G_F}{\sqrt{2}}C_{7\gamma}^e(\Lambda) &= -i\Lambda^{-2}(V_{ts}^*V_{tb})^{-1}\left\{(\eta_{\tilde{b}'}^L)^\dagger_{s\tilde{X}^j}(\eta_{\tilde{b}'}^L)_{\tilde{X}^jb}F_{1,\gamma}^{(e)}(x_{\tilde{X}^j},x_{\tilde{b}'})+\frac{m_f}{m_b}(\eta_{\tilde{b}'}^L)^\dagger_{s\tilde{X}^j}(\eta_{\tilde{b}'}^R)_{\tilde{X}^jb}F_{2,\gamma}^{(e)}(x_{\tilde{X}^j},x_{\tilde{b}'})\right\}, \\ \frac{G_F}{\sqrt{2}}\tilde{C}_{7\gamma}^e(\Lambda) &= \frac{G_F}{\sqrt{2}}C_{7\gamma}^e(\Lambda)(\eta_{\tilde{b}'}^L \leftrightarrow \eta_{\tilde{b}'}^R).\end{aligned}\quad (19)$$

$$\begin{aligned}F_{1,\gamma}^{(e)}(x,y) &= \left[-\frac{1}{72}\frac{\partial^3\varrho_{3,1}}{\partial^3y}+\frac{1}{24}\frac{\partial^2\varrho_{2,1}}{\partial^2y}\right](x,y), \\ F_{2,\gamma}^{(e)}(x,y) &= \left[-\frac{1}{12}\frac{\partial^2\varrho_{2,1}}{\partial^2y}+\frac{1}{6}\frac{\partial\varrho_{1,1}}{\partial y}\right](x,y).\end{aligned}\quad (20)$$

From Figure 1.(f), we obtain the corrections from gluinos Λ_G in MSSM, the Wilson coefficients at μ_{EW} are

$$\begin{aligned}\frac{G_F}{\sqrt{2}}C_{7\gamma}^f(\Lambda) &= -i\Lambda^{-2}(V_{ts}^*V_{tb})^{-1}\left\{(\eta_{\tilde{D}}^L)^\dagger_{s\Lambda_G}(\eta_{\tilde{D}}^L)_{\Lambda_G b}F_{1,\gamma}^{(f)}(x_{\Lambda_G},x_{\tilde{D}})+\frac{m_f}{m_b}(\eta_{\tilde{D}}^L)^\dagger_{s\Lambda_G}(\eta_{\tilde{D}}^R)_{\Lambda_G b}F_{2,\gamma}^{(f)}(x_{\Lambda_G},x_{\tilde{D}})\right\}, \\ \frac{G_F}{\sqrt{2}}\tilde{C}_{7\gamma}^f(\Lambda) &= \frac{G_F}{\sqrt{2}}C_{7\gamma}^f(\Lambda)(\eta_{\tilde{D}}^L \leftrightarrow \eta_{\tilde{D}}^R).\end{aligned}\quad (21)$$

with

$$\begin{aligned}
F_{1,\gamma}^{(f)}(x, y) &= \left[\frac{1}{24} \frac{\partial^3 \varrho_{3,1}}{\partial^3 y} - \frac{1}{8} \frac{\partial^2 \varrho_{2,1}}{\partial^2 y} \right](x, y), \\
F_{2,\gamma}^{(f)}(x, y) &= \left[\frac{1}{4} \frac{\partial^2 \varrho_{2,1}}{\partial^2 y} - \frac{1}{2} \frac{\partial \varrho_{1,1}}{\partial y} \right](x, y).
\end{aligned} \tag{22}$$

The corrections to C_{8g} and \tilde{C}_{8g} at electroweak scale can be obtained by attaching the gluon to intermediate virtual particles with colors. For diagrams in Figure 1, the gluon can be attached to SM up-type quarks u_i , squarks in MSSM \tilde{U}, \tilde{D} , exotic quarks b' with charge $-1/3$ and its supersymmetric partners \tilde{b}' , as well as the gluinos Λ_G . Wilson coefficients at electroweak scale can be formulated as:

$$\begin{aligned}
\frac{G_F}{\sqrt{2}} C_{8G}^a(\Lambda) &= -i\Lambda^{-2} (V_{ts}^* V_{tb})^{-1} \left\{ (\eta_{H^\pm}^L)^\dagger_{su_i} (\eta_{H^\pm}^L)_{u_i b} F_{1,g}^{(a)}(x_{u_i}, x_{H^\pm}) + \frac{m_f}{m_b} (\eta_{H^\pm}^L)^\dagger_{su_i} (\eta_{H^\pm}^R)_{u_i b} F_{2,g}^{(a)}(x_{u_i}, x_{H^\pm}) \right\}, \\
\frac{G_F}{\sqrt{2}} \tilde{C}_{8G}^a(\Lambda) &= \frac{G_F}{\sqrt{2}} C_{8G}^a(\Lambda) (\eta_{H^\pm}^L \leftrightarrow \eta_{H^\pm}^R, \eta_{G^\pm}^L \leftrightarrow \eta_{G^\pm}^R), \\
\frac{G_F}{\sqrt{2}} C_{8G}^b(\Lambda) &= -i\Lambda^{-2} (V_{ts}^* V_{tb})^{-1} \left\{ (\xi_{\chi_i^0}^L)^\dagger_{s\tilde{D}} (\xi_{\chi_i^0}^L)_{\tilde{D}b} F_{1,g}^{(b)}(x_{\chi_i^0}, x_{\tilde{D}}) + \frac{m_f}{m_b} (\xi_{\chi_i^0}^L)^\dagger_{s\tilde{D}} (\xi_{\chi_i^0}^R)_{\tilde{D}b} F_{2,g}^{(b)}(x_{\chi_i^0}, x_{\tilde{D}}) \right. \\
&\quad \left. + (\xi_{\chi_B^0}^L)^\dagger_{s\tilde{D}} (\xi_{\chi_B^0}^L)_{\tilde{D}b} F_{1,g}^{(b)}(x_{\chi_B^0}, x_{\tilde{D}}) + \frac{m_f}{m_b} (\xi_{\chi_B^0}^L)^\dagger_{s\tilde{D}} (\xi_{\chi_B^0}^R)_{\tilde{D}b} F_{2,g}^{(b)}(x_{\chi_B^0}, x_{\tilde{D}}) \right\}, \\
\frac{G_F}{\sqrt{2}} \tilde{C}_{8G}^b(\Lambda) &= \frac{G_F}{\sqrt{2}} C_{8G}^b(\Lambda) (\xi_{\chi_i^0}^L \leftrightarrow \xi_{\chi_i^0}^R, \xi_{\chi_B^0}^L \leftrightarrow \xi_{\chi_B^0}^R), \\
\frac{G_F}{\sqrt{2}} C_{8G}^c(\Lambda) &= -i\Lambda^{-2} (V_{ts}^* V_{tb})^{-1} \left\{ (\xi_{\chi_i^\pm}^L)^\dagger_{s\tilde{D}} (\xi_{\chi_i^\pm}^L)_{\tilde{D}b} F_{1,g}^{(c)}(x_{\chi_i^\pm}, x_{\tilde{U}}) + \frac{m_f}{m_b} (\xi_{\chi_i^\pm}^L)^\dagger_{s\tilde{D}} (\xi_{\chi_i^\pm}^R)_{\tilde{D}b} F_{2,g}^{(c)}(x_{\chi_i^\pm}, x_{\tilde{U}}) \right\}, \\
\frac{G_F}{\sqrt{2}} \tilde{C}_{8G}^c(\Lambda) &= \frac{G_F}{\sqrt{2}} C_{8G}^c(\Lambda) (\xi_{\chi_i^\pm}^L \leftrightarrow \xi_{\chi_i^\pm}^R), \\
\frac{G_F}{\sqrt{2}} C_{8G}^d(\Lambda) &= -i\Lambda^{-2} (V_{ts}^* V_{tb})^{-1} \left\{ (\eta_{X^j}^L)^\dagger_{sb'} (\eta_{X^j}^L)_{b'b} F_{1,g}^{(d)}(x_{b'}, x_{X^j}) + \frac{m_f}{m_b} (\eta_{X^j}^L)^\dagger_{sb'} (\eta_{X^j}^R)_{b'b} F_{2,g}^{(d)}(x_{b'}, x_{X^j}) \right\}, \\
\frac{G_F}{\sqrt{2}} \tilde{C}_{8G}^d(\Lambda) &= \frac{G_F}{\sqrt{2}} C_{8G}^d(\Lambda) (\eta_{X^j}^L \leftrightarrow \eta_{X^j}^R), \\
\frac{G_F}{\sqrt{2}} C_{8G}^e(\Lambda) &= -i\Lambda^{-2} (V_{ts}^* V_{tb})^{-1} \left\{ (\xi_{\tilde{b}'}^L)^\dagger_{s\tilde{X}^j} (\xi_{\tilde{b}'}^L)_{\tilde{X}^j b} F_{1,g}^{(e)}(x_{\tilde{X}^j}, x_{\tilde{b}'}) + \frac{m_f}{m_b} (\xi_{\tilde{b}'}^L)^\dagger_{s\tilde{X}^j} (\xi_{\tilde{b}'}^R)_{\tilde{X}^j b} F_{2,g}^{(e)}(x_{\tilde{X}^j}, x_{\tilde{b}'}) \right\}, \\
\frac{G_F}{\sqrt{2}} \tilde{C}_{8G}^e(\Lambda) &= \frac{G_F}{\sqrt{2}} C_{8G}^e(\Lambda) (\xi_{\tilde{b}'}^L \leftrightarrow \xi_{\tilde{b}'}^R),
\end{aligned} \tag{23}$$

with the form factors listed below. As gluon can only be attached to intermediate fermion u_i and b' in Figure 1.(a) and 1.(d), so the form factors have the same expressions. While in Figure 1.(b), 1.(c) and Figure 1.(e), the gluon can only be attached to scalar particles. Then form factors associated to these diagrams are the same. By summing over the contributions

to Wilson coefficients when gluon attached to Λ_G and \tilde{D} , we get form factors of Figure 1.(f).

$$\begin{aligned}
F_{1,g}^{(a)}(x, y) &= F_{1,g}^{(d)}(x, y) = \left[-\frac{1}{24} \frac{\partial^3 \varrho_{3,1}}{\partial^3 y} + \frac{1}{4} \frac{\partial^2 \varrho_{2,1}}{\partial^2 y} - \frac{1}{4} \frac{\partial \varrho_{1,1}}{\partial y} \right] (x, y), \\
F_{2,g}^{(a)}(x, y) &= F_{2,g}^{(d)}(x, y) = \left[-\frac{1}{4} \frac{\partial^2 \varrho_{2,1}}{\partial^2 y} + \frac{1}{2} \frac{\partial \varrho_{1,1}}{\partial y} - \frac{1}{2} \frac{\partial \varrho_{1,1}}{\partial x} \right] (x, y), \\
F_{1,g}^{(b)}(x, y) &= F_{1,g}^{(c)}(x, y) = F_{1,g}^{(e)}(x, y) = \left[\frac{1}{24} \frac{\partial^3 \varrho_{3,1}}{\partial^3 y} - \frac{1}{8} \frac{\partial^2 \varrho_{2,1}}{\partial^2 y} \right] (x, y), \\
F_{2,g}^{(b)}(x, y) &= F_{2,g}^{(c)}(x, y) = F_{2,g}^{(e)}(x, y) = \left[\frac{1}{4} \frac{\partial^2 \varrho_{2,1}}{\partial^2 y} - \frac{1}{2} \frac{\partial \varrho_{1,1}}{\partial y} \right] (x, y), \\
F_{1,g}^{(f)}(x, y) &= \left[\frac{1}{8} \frac{\partial^2 \varrho_{2,1}}{\partial^2 y} - \frac{1}{4} \frac{\partial \varrho_{1,1}}{\partial y} \right] (x, y), \\
F_{2,g}^{(f)}(x, y) &= \left[-\frac{1}{2} \frac{\partial \varrho_{1,1}}{\partial x} \right] (x, y).
\end{aligned} \tag{24}$$

The Wilson coefficients obtained above can also be used to direct CP-violation in $\bar{B} \rightarrow X_s \gamma$ and the time-dependent CP-asymmetry in $B \rightarrow K^* \gamma$. The direct CP-violation $A_{\bar{B} \rightarrow X_s \gamma}^{CP}$ and CP-asymmetry $S_{K^* \gamma}$ are defined in hadronic scale [22–26]

$$\begin{aligned}
A_{\bar{B} \rightarrow X_s \gamma}^{CP} &= \frac{\Gamma(\bar{B} \rightarrow X_s \gamma) - \Gamma(B \rightarrow X_{\bar{s}} \gamma)}{\Gamma(\bar{B} \rightarrow X_s \gamma) + \Gamma(B \rightarrow X_{\bar{s}} \gamma)} \Big|_{E_\gamma > (1-\delta) E_\gamma^{max}} \\
&\simeq \frac{10^{-2}}{|C_7(\mu_b)|^2} \left[1.23 \Im(C_2(\mu_b) C_7^*(\mu_b)) \right. \\
&\quad \left. - 9.52 \Im(C_8(\mu_b) C_7^*(\mu_b)) + 0.01 \Im(C_2(\mu_b) C_8^*(\mu_b)) \right],
\end{aligned} \tag{25}$$

$$S_{K^* \gamma} \simeq \frac{2 \text{Im}(e^{-i\phi_d} C_7(\mu_b) C_7'(\mu_b))}{|C_7(\mu_b)|^2 + |C_7'(\mu_b)|^2}, \tag{26}$$

where the photon energy cut in A^{CP} is taken as $\delta = 3$, and ϕ_d in $S_{K^* \gamma}$ is phase of B_d mixing amplitude. Here we use the experimental data $\sin \phi_d = 0.67 \pm 0.02$ given in ref. [27].

As the Wilson coefficients are calculated at electroweak scale μ_{EW} , we need to evolve them down to hadronic scale $\mu \sim m_b$ with renormalization group equations.

$$\begin{aligned}
\vec{C}_{NP}(\mu) &= \hat{U}(\mu, \mu_0) \vec{C}_{NP}(\mu_0), \\
\vec{C}'_{NP}(\mu) &= \hat{U}'(\mu, \mu_0) \vec{C}'_{NP}(\mu_0),
\end{aligned} \tag{27}$$

where the Wilson coefficients are constructed as

$$\begin{aligned}
\vec{C}_{NP}^T &= (C_{1,NP}, \dots, C_{6,NP}, C_{7,NP}^{eff}, C_{8,NP}^{eff}), \\
\vec{C}'_{NP}{}^T &= (C_{7,NP}^{eff}, C_{8,NP}^{eff}).
\end{aligned} \tag{28}$$

To be convenient, we take the numerical results of effective coefficients C^{eff} from SM at next-to-next-to-leading logarithmic(NNLL) level, $C_7^{eff}(m_b) = -0.304$, $C_8^{eff}(m_b) = -0.167$. The evolving matrices involved in Eq.(27) are given as

$$\begin{aligned}\hat{U}(\mu, \mu_0) &\simeq 1 - \left[\frac{1}{2\beta_0} \ln \frac{\alpha_s(\mu)}{\alpha_s(\mu_0)} \right] \hat{\gamma}^{(0)T}, \\ \hat{U}'(\mu, \mu_0) &\simeq 1 - \left[\frac{1}{2\beta_0} \ln \frac{\alpha_s(\mu)}{\alpha_s(\mu_0)} \right] \hat{\gamma}'^{(0)T},\end{aligned}\tag{29}$$

with anomalous dimension matrices

$$\hat{\gamma}^{(0)} = \begin{pmatrix} -4 & \frac{8}{3} & 0 & -\frac{2}{9} & 0 & 0 & -\frac{208}{243} & \frac{173}{162} \\ 12 & 0 & 0 & \frac{4}{3} & 0 & 0 & \frac{416}{81} & \frac{70}{27} \\ 0 & 0 & 0 & -\frac{52}{3} & 0 & 2 & -\frac{176}{81} & \frac{14}{27} \\ 0 & 0 & -\frac{40}{9} & -\frac{100}{9} & \frac{4}{9} & \frac{5}{6} & -\frac{152}{243} & -\frac{587}{162} \\ 0 & 0 & 0 & -\frac{256}{3} & 0 & 20 & -\frac{6272}{81} & \frac{6596}{27} \\ 0 & 0 & -\frac{256}{9} & \frac{56}{9} & \frac{40}{9} & -\frac{2}{3} & \frac{4624}{243} & \frac{4772}{81} \\ 0 & 0 & 0 & 0 & 0 & 0 & \frac{32}{3} & 0 \\ 0 & 0 & 0 & 0 & 0 & 0 & -\frac{32}{9} & \frac{28}{3} \end{pmatrix},\tag{30}$$

and

$$\hat{\gamma}'^{(0)} = \begin{pmatrix} \frac{32}{3} & 0 \\ -\frac{32}{9} & \frac{28}{3} \end{pmatrix}.\tag{31}$$

IV. NUMERICAL ANALYSIS

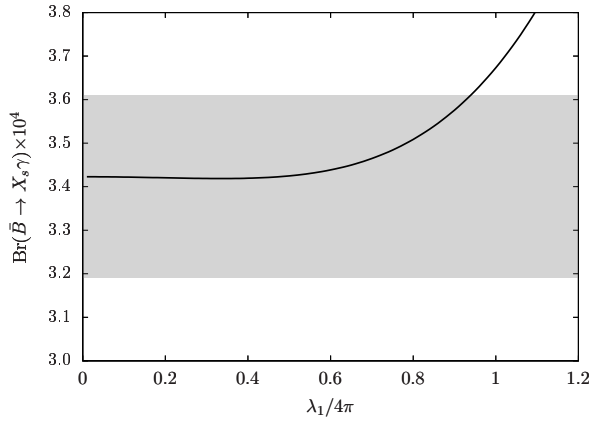
The consistency of SM prediction and experimental data on $\bar{B} \rightarrow X_s \gamma$ sets stringent constraint on new physics parameters. In this section, we discuss the numerical results of branching ratio with some assumptions. The SM inputs are given in Table II. All the parameters with mass dimension are given in the unit GeV. To be concise, we omit all the unit GeV in this section. Other free parameters introduced in BLMSSM are set to be $A_{BU} = A_{BD} = A_{BQ} = A'_{BU} = A'_{BD} = A'_{BQ} = A_{d_4} = A_{d_5} = A_{u_4} = A_{u_5} = A'_{d_4} = A'_{d_5} = A'_{u_4} = A'_{u_5} = 100$, $M_{\hat{Q}_4}^2 = M_{\hat{Q}_5}^2 = M_{\hat{U}_4}^2 = M_{\hat{U}_5}^2 = M_{\hat{D}_4}^2 = M_{\hat{D}_5}^2 = 2500$, $m_1 = m_2 = 1200$ and $m_{Z_B} = 1000$ to make sure the masses of new physics particles under experimental limitations.

As a new field introduced in BLMSSM, superfield X interacts with exotic quarks. The couplings between X and \hat{Q}_5, \hat{U}_5 denoted by λ_i , ($i = 1, 2, 3$) are given in Eq.4. From the

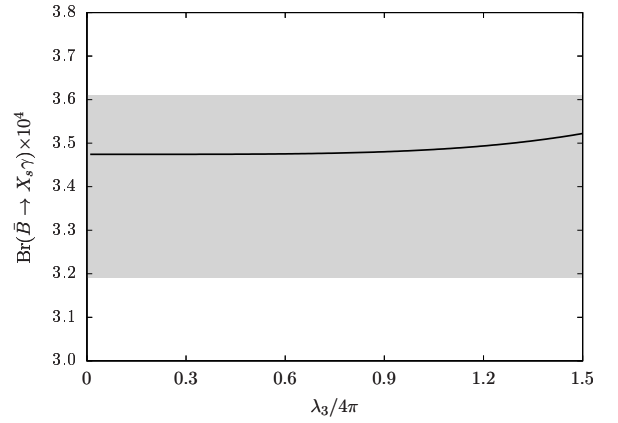
analytical expressions, one can find the Wilson coefficients are sensitive to these couplings as well as coefficients of mass term of X , which turns up in \mathcal{W}_X as μ_X and B_X . We show the branching ratio varying with λ_1 , λ_3 , μ_X and B_X in figure 2. The dependency of λ_2 is not listed as it is similar to λ_1 .

TABLE II: SM inputs in numerical analysis.

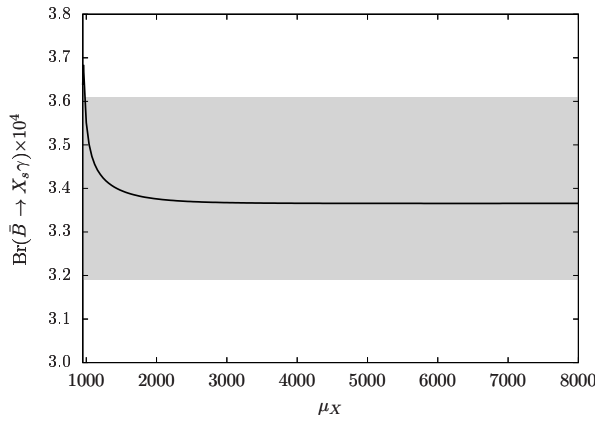
α	1/128	m_W	80.385	m_Z	91.188
m_u	0.0023	m_c	1.275	m_t	173.5
m_d	0.0048	m_s	0.095	m_b	4.18



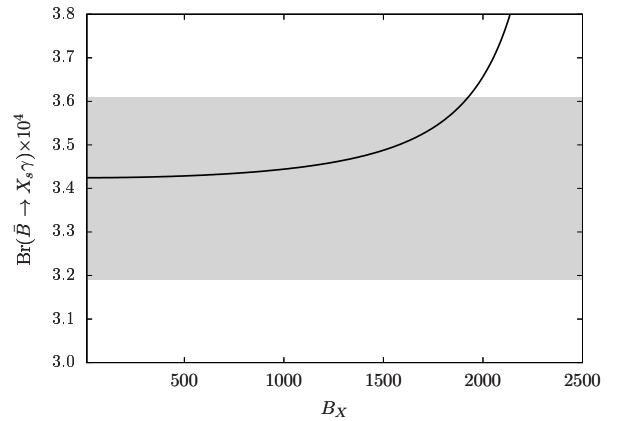
(a)



(b)



(c)



(d)

FIG. 2: $Br(\bar{B} \rightarrow X_s \gamma)$ varying with parameters relevant to superfield X .

In Figure 2.(a), one can find the branching ratio increases when λ_1 raises up. The experi-

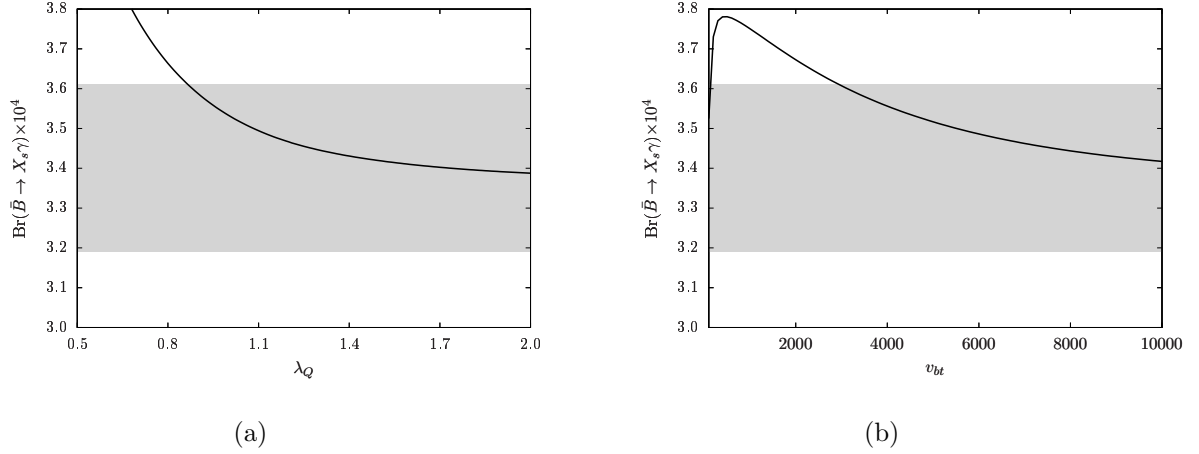


FIG. 3: $Br(\bar{B} \rightarrow X_s \gamma)$ varying with λ_Q and v_{bt} .

mental limitations are denoted by the gray area, and we have taken $\lambda_3/(4\pi) = 0.07$, $\tan \beta = 10$, $\lambda_Q = 0.7$, $\lambda_U = 0.3$, $\lambda_D = 0.2$, $\mu = -600$, $\mu_B = \mu_X = m_{Z_B} = m_B = 1000$, $B_X = 400$, $v_{bt} = 6000$. It can be seen in this figure that branching ratio reaches the upper limitations of experimental limitations when $\lambda_1/(4\pi) \sim 0.94$, then we get the constrain $\lambda_1/(4\pi) < 0.94$.

Similarly, we plot the branching ratio varying with λ_3 in Figure 2.(b). By taking $\lambda_1/(4\pi) = 0.07$, which satisfies the limitations obtained in Figure 2.(a), and $\tan \beta = 5$, $\lambda_Q = 0.2$, $\lambda_U = 0.5$, $\lambda_D = 0.8$, $\mu = -800$, $\mu_B = \mu_X = 1100$, $m_{Z_B} = 1000$, $m_B = 500$, $B_X = 400$, $v_{bt} = 6000$, we find the branching ratio rises very slowly when $\lambda_3/(4\pi)$ runs from 0.01 to 1.5. The whole curve lies in the gray area, which means the branching ratio satisfies the experimental constraint under our assumptions.

To investigate the trends of $Br(\bar{B} \rightarrow X_s \gamma)$ varying with μ_X , we take $\lambda_1/(4\pi) = 0.06$, $\lambda_3/(4\pi) = 0.08$, $\tan \beta = 5$, $\lambda_Q = 0.8$, $\lambda_U = 0.5$, $\lambda_D = 0.2$, $\mu = -600$, $\mu_B = 1000$, $B_X = 400$, $m_{z_B} = 1100$, $v_{bt} = 6000$, $m_B = 2500$. We find from Figure 2.(c) that the branching ratio diminishes steeply with increasing of μ_X , and finally gets to the value of standard model. In Figure 2.(d), we plot the branching ratio varying with B_X , where we take $\lambda_1/(4\pi) = 0.15$, $\lambda_3/(4\pi) = 0.08$, $\tan \beta = 5$, $\lambda_Q = 0.7$, $\lambda_U = 0.2$, $\lambda_D = 0.3$, $\mu = -1000$, $\mu_B = 1100$, $\mu_X = 2500$, $m_{z_B} = 900$, $v_{bt} = 5500$, $m_B = 2000$. With the upper limitations of experimental result, we get the constraints $B_X < 1930$.

In Figure 3.(a), we present the branching ratio varying with λ_Q , which is the coupling turns up in superpotential term $\lambda_Q \hat{Q}_4 \hat{Q}_5^c \hat{\Phi}_B$. With $\lambda_1/(4\pi) = 0.08$, $\lambda_3/(4\pi) = 0.06$, $\tan \beta = 20$, $\lambda_U = 0.3$, $\lambda_D = 0.6$, $\mu = -800$, $\mu_B = \mu_X = 1000$, $B_X = 400$, $m_{z_B} = 1000$, $v_{bt} =$

5000, $m_B = 1500$, we find branching ratio decreases when λ_Q gets larger. To consist with the experimental data, one has $\lambda_Q > 0.87$. Another interesting parameter is v_{bt} , which is defined as $v_{bt} = \sqrt{\bar{v}_B^2 + v_B^2}$, where v_B and \bar{v}_B are VEVs of Φ_B and φ_B respectively. We plot branching ratio varying with v_{bt} in Figure 3.(b) with $\lambda_1/(4\pi) = \lambda_3/(4\pi) = 0.1$, $\tan \beta = 5$, $\lambda_Q = 0.4$, $\lambda_U = 0.2$, $\lambda_D = 0.7$, $\mu = -1000$, $\mu_B = 1100$, $\mu_X = 1500$, $B_X = 400$, $m_{z_B} = 1000$, $m_B = 1500$. To satisfy the experimental constraints, we have $v_{bt} > 2900$.

Additionally, we plot the direct CP-violation of $\bar{B} \rightarrow X_s \gamma$ and time-dependent CP-asymmetry of $B \rightarrow K^* \gamma$ varying with $\lambda_1, \lambda_3, \mu_X, B_X, \lambda_Q, \lambda_D$ and v_{bt} . Within the framework of SM, we have $-0.6\% < A_{CP}^{SM} < +2.8\%$ [28], and the average value of this observable is $A_{CP}^{exp} = -0.009 \pm 0.018$ [1]. Within some uncertainty, the theoretical value is consistent with the experimental result. Compared with direct CP-violation of $\bar{B} \rightarrow X_s \gamma$, there is significant deviation between SM prediction and experimental result of $S_{K^* \gamma}$. The SM prediction of time-dependent CP-asymmetry in $B \rightarrow K^* \gamma$ at LO level is given as $S_{K^* \gamma}^{SM} \simeq (-2.3 \pm 1.6)\%$ [29] and the experimental result is $S_{K^* \gamma} \simeq -0.15 \pm 0.22$ [1, 19].

To investigate $A_{\bar{B} \rightarrow X_s \gamma}^{CP}$ and $S_{K^* \gamma}$ numerically, some parameters are taken to be complex, and the area within experimental boundaries are filled to be gray in the presented figures. In Figure 4, we plot the dependency of parameters relevant to superfield X . Under our assumptions of free parameters introduced in BLMSSM, we find that $A_{\bar{B} \rightarrow X_s \gamma}^{CP}$ (solid line) are hardly affected by the change of $\lambda_1, \lambda_3, \mu_X, B_X$. Though corrections from one-loop level are almost zero, the numerical results are consistent with experimental data.

As shown in Figure 4.(a), one-loop corrections to $S_{K^* \gamma}$ (dashed line) in BLMSSM can reach -0.25 with appropriate inputs. By changing the free parameters, one finds $S_{K^* \gamma}$ can be as small as zero in Figure 4.(b). In Figure 4.(c), it can be seen that $S_{K^* \gamma}$ raise obviously with increasing of μ_X , and finally gets stable around zero. The $S_{K^* \gamma}$ varying with B_X are given in Figure 4.(d). When B_X raises up, we can see that $S_{K^* \gamma}$ decreases. Within the range of parameters $\lambda_1, \lambda_3, \mu_X$ and B_X , we find $S_{K^* \gamma}$ is consistent with experimental data.

In Figure 5, we take into account the parameters λ_Q and λ_D . When λ_Q runs from 0.01 to 2.0, the time-dependent CP-asymmetry decrease from 0.02 to -0.22 . While for the increasing of λ_D , $S_{K^* \gamma}$ raises from -0.28 to -0.02 . Under our assumptions, we conclude that λ_Q and λ_D affect $S_{K^* \gamma}$ apparently, and the numerical results of new physics correction are consistent with experimental data. However, the direct CP-violation of $\bar{B} \rightarrow X_s \gamma$ depends on λ_Q and λ_D weakly, and the one-loop contributions from BLMSSM are very small.

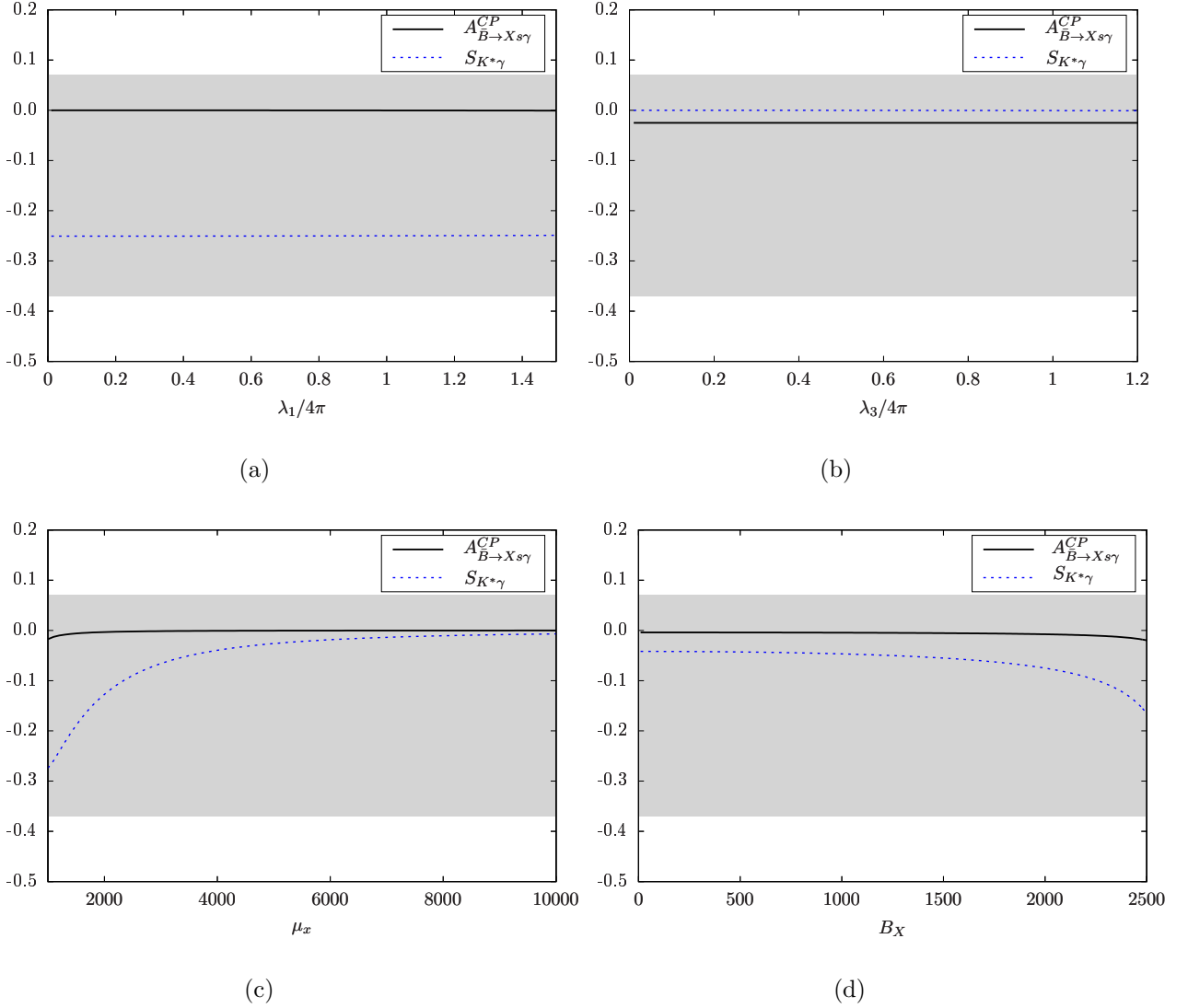


FIG. 4: $A_{\bar{B} \rightarrow X s \gamma}^{CP}$ and $S_{K^* \gamma}$ varying with parameters relevant to superfield X .

The last Figure 6 illustrates the trend of $S_{K^* \gamma}$ and $A_{\bar{B} \rightarrow X s \gamma}^{CP}$ varying with v_{bt} . By taking $\lambda_1/(4\pi) = 0.8, \lambda_3/(4\pi) = 0.9, B_X = 400$ and $\lambda_Q = 0.4e^{0.625\pi}$, we find that $S_{K^* \gamma}$ increases from -0.26 to -0.06 . The $A_{\bar{B} \rightarrow X s \gamma}^{CP}$ stays around zero within the range $100 < v_{bt} < 10000$.

V. CONCLUSIONS

As an interesting process of FCNC, we investigate the transition $b \rightarrow s\gamma$ within the framework of BLSSM. With effective Hamiltonian method, we present the Wilson coefficients extracted from amplitudes corresponding to the concerned one-loop diagrams. Based

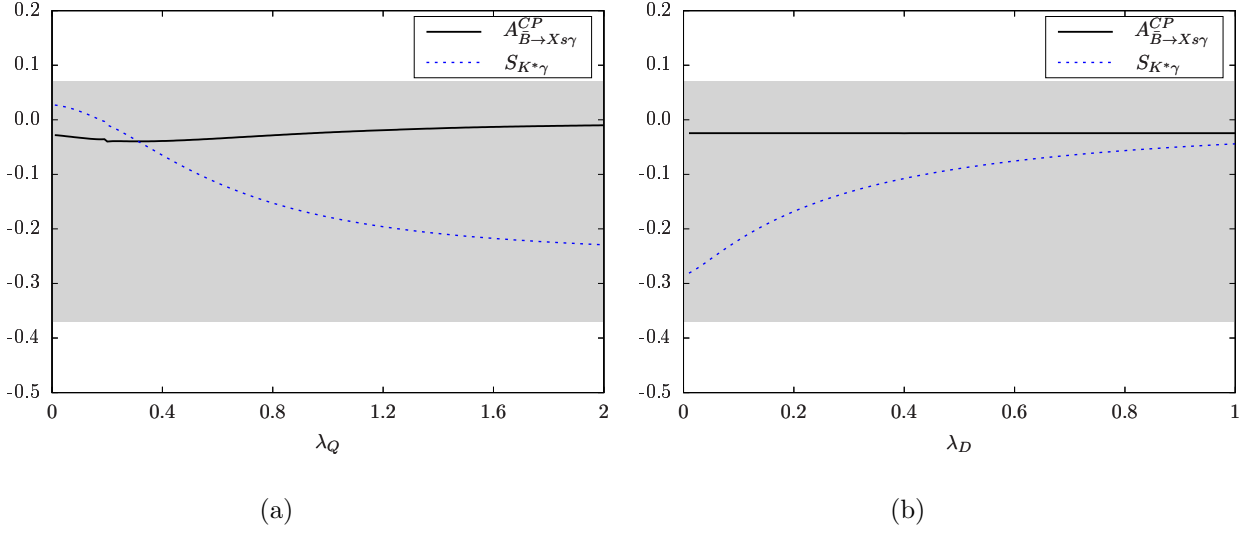


FIG. 5: $A_{\bar{B} \rightarrow X_s \gamma}^{CP}$ and $S_{K^* \gamma}$ varying with λ_Q and λ_D .

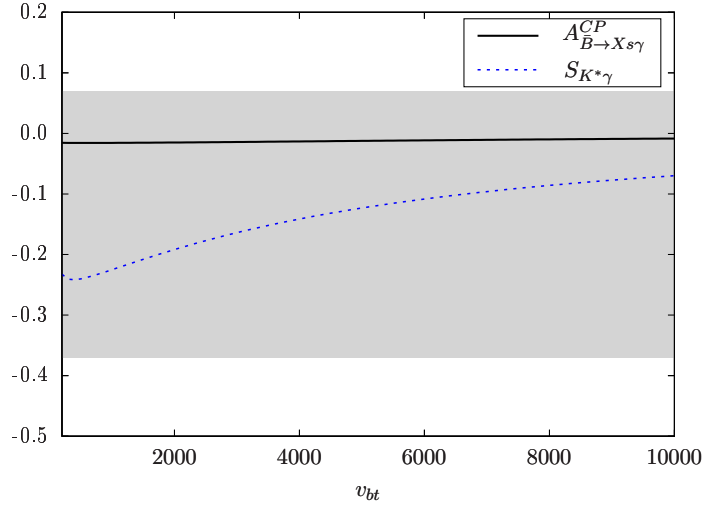


FIG. 6: $A_{\bar{B} \rightarrow X_s \gamma}^{CP}$ and $S_{K^* \gamma}$ varying with v_{bt} .

on the analytical expressions, constraints on parameters are given in the numerical section with the experimental data of branching ratio of $\bar{B} \rightarrow X_s \gamma$. The direct CP-violation of $\bar{B} \rightarrow X_s \gamma$ in BLMSSM is very small, and depend on the free parameters weakly. However, the time-dependent CP-asymmetry $S_{K^* \gamma}$ in $B \rightarrow K^* \gamma$ varies with $\mu_X, B_X, \lambda_Q, \lambda_D$ and v_{bt} obviously. The contributions from new physics can reach -0.28 under appropriate setup of

the parameters.

-
- [1] M. Tanabashi et al.(Particle Data Group), Phys. Rev. D 98: 030001 (2018)
 - [2] M. Misiak et al., Phys. Rev. Lett. 114: 221801 (2015)
 - [3] M. Czakon, P. Fiedler, T. Huber, M. Misiak, T. Schutzmeier and M. Steinhauser, (2015), arXiv:1503.01791[hep-ph]
 - [4] M. Misiak et al., Phys. Rev. Lett. 98: 022002 (2007)
 - [5] M. Misiak and M. Steinhauser, Nucl. Phys. B 764: 62 (2007)
 - [6] K. Chetyrkin, M. Misiak and M. Munz, Phys. Lett. B 400: 206 (1997)
 - [7] C. Greub, T. Hurth and D. Wyler, Phys. Rev. D 54: 3350 (1996)
 - [8] K. Adel and Y.-P. Yao, Phys. Rev. D 49: 4945 (1994)
 - [9] A. Ali and C. Greub, Phys. Lett. B 361: 146 (1995)
 - [10] J. Rosiek, Phys. Rev. D 41: 3464 (1990)
 - [11] P. F. Perez and M. B. Wise, JHEP, 1108: 068 (2011)
 - [12] P. F. Perez and M. B. Wise, Phys. Rev. D 82: 011901 (2010)
 - [13] P. F. Perez, Physics reports 597: 1 (2015)
 - [14] S. M. Zhao, T.F. Feng, H.B.Zhang, B. Yan and Y. J. Zhang, JHEP,1411: 119 (2014)
 - [15] S. M. Zhao, T. F. Feng, Z. J. Yang, H. B. Zhang, X. X. Dong and T. Guo, Eur. Phys. J. C77: 102 (2017)
 - [16] T. F. Feng, S. M. Zhao, H. B. Zhang, Y. J. Zhang, Y. L. Yan, Nucl. Phys. B 871: 223 (2013)
 - [17] H. Li, J. B. Chen and L. L. Xing, MPLA 33: 1850034 (2018)
 - [18] E. Lunghi and J. Matias, JHEP 0704:058 (2007)
 - [19] T. F. Feng, Y. L. Yan, H. B. Zhang and S. M. Zhao, Phys. Rev. D 92 : 055024 (2015)
 - [20] C. Bobeth, M. Misiak and J. Urban, Nucl. Phys. B 574:291-330 (2000)
 - [21] W. Altmannshofer, P. Ball1, A. Bharucha, A. J. Buras, D. M. Straub1 and M. Wick, JHEP 01:019 (2009)
 - [22] H. M. Asatrian and A. N. Ioannissian, Phys. Rev. D 54 (1996) 5642
 - [23] M. Ciuchini, E. Gabrielli and G.F. Giudice, Phys. Lett. B388:353 (1996)
 - [24] S. Baek, P. Ko, Phys. Rev. Lett. 83:488 (1999)
 - [25] A. L. Kagan and M. Neubert, Phys. Rev. D 58:094012 (1998)

- [26] K. Kiers, A. Soni, and G. H. Wu, Phys. Rev. D62:116004 (2000)
- [27] D. Asner et al.(Heavy Flavor Averaging Group), (2010) arXiv:1010.1589[hep-ex]
- [28] M. Benzke, S. J. Lee, M. Neubert and G. Paz, Phys. Rev. Lett. 106:141801 (2011)
- [29] P. Ball, G. W. Jones and R. Zwicky Phys. Rev. D 75:054004 (2007)